JOURNAL OF GUIDANCE, CONTROL, AND DYNAMICS
Vol. 20, No. 1, January–February 1997

Estimation of Vehicle Dynamic and Static Parameters from Magnetometer Data

John F. Kinkel* and Mitchell Thomas†
L'Garde, Inc., Tustin, California 92780-6487

A method of estimating the spin rate, coning rate, and coning half-angle of a spinning space vehicle using the data from a single-axis magnetometer mounted transversely to the spin axis of the vehicle is described. In addition, estimates are available for the angle between the total angular momentum vector of the vehicle and the local magnetic field vector. The ratio of the spin axis to transverse axes moments of inertia may also be calculated. Estimates for several other parameters, including the local magnetic field intensity, are available. An example is given for a magnetometer mounted in a laboratory fixture to provide spin and coning motion. Finally, the use of the data to obtain absolute pointing information is illustrated, including an error analysis.

Introduction

FOR low-budget space experiments we desire to provide as much data as possible regarding the dynamics of a spinning vehicle while satisfying severe constraints on the size, weight, power, and cost of the instrumentation package. As demonstrated in this paper, a single-axis magnetometer mounted transversely to the spin axis of the vehicle provides a great deal of information when the data are appropriately processed. Although the technique has been demonstrated to work for real data (a sample problem is included here), the existence of a unique solution has not been proven.

Deduction of Dynamics Parameters

We show how the magnetometer data will provide estimates for several parameters describing the vehicle dynamics. The basic approach is to formulate a parameter estimation problem based on a mathematical model (the estimation model) representing the motion of the vehicle-mounted magnetometer. The parameter set in the estimation model includes several parameters of interest in the space experiment, e.g., the vehicle spin rate, coning rate, coning half-angle, and other parameters to be described. Loosely speaking, the problem is to determine the model parameter set that minimizes (in some sense) the difference (distance) between the model magnetometer data stream and the actual magnetometer data stream. A nonlinear programming algorithm is used to perform the required minimization. The details of the problem formulation and solution are described in the sequel.

Estimation Problem

There is a strong connection between estimation and approximation. For our present purposes we prefer to use the approximation problem formulation described by Rice.[1]

After a flight of the magnetometer, we are given a data sequence $f(t_i)$. We devise an estimation model $F(\boldsymbol{\alpha}, t_i)$ incorporating a vector $\boldsymbol{\alpha}$ whose elements comprise the set of parameters to be estimated. The problem is to find the optimal estimate for α that minimizes the distance between $f(t_i)$ and $F(\boldsymbol{\alpha}, t_i)$. Thus, where

$f(t_i) =$ measurement data sequence
$F(\boldsymbol{\alpha}, t_i) =$ estimation model data sequence
$\boldsymbol{\alpha} =$ model parameter vector

the optimal estimation problem can be summarized as

$$\rho[F(\hat{\boldsymbol{\alpha}}, t_i) - f(t_i)] \leq \rho[F(\boldsymbol{\alpha}, t_i) - f(t_i)] \tag{1}$$

where

$\rho(\cdot) =$ distance function[2,3]
$\hat{\boldsymbol{\alpha}} =$ optimal estimate for parameter vector

To make use of this basic problem formulation, it is necessary to do the following.

1) Define the estimation model $F(\boldsymbol{\alpha}, t_i)$ and associated parameter vector $\boldsymbol{\alpha}$.

2) Define the distance function ρ.

3) Provide a means of solving the minimization problem.

The next section defines the estimation model.

For convenience, we use a least-squares solution.[1–4] We define

$$z(\boldsymbol{\alpha}) = \sum_{i=1}^{n} [F(\boldsymbol{\alpha}, t_i) - f(t_i)]^2 \tag{2}$$

Then, the optimal estimate for $\boldsymbol{\alpha}$ is defined by

$$z(\hat{\boldsymbol{\alpha}}) \leq z(\boldsymbol{\alpha}) \tag{3}$$

We may apply a nonlinear programming algorithm to solve the minimization problem.[5–9]

Estimation Model

We assume that the vehicle is symmetrical about the spin axis, which we designate as the z axis; i.e., we assume that $I_X = I_Y$ and $I_{XY} = I_{XZ} = I_{YZ} = 0$, where the I designates the moments of inertia indicated by the subscripts.

Using the notation of Hughes[10] we may write the output of the magnetometer as the dot product of the magnetometer sensitivity vector and the local magnetic intensity vector, namely,

$$F_o = \boldsymbol{u} \cdot \boldsymbol{h} \tag{4}$$

where

$F_o =$ magnetometer output
$\boldsymbol{u} =$ magnetometer sensitivity vector
$\boldsymbol{h} =$ local magnetic field vector, G

We will use a standard set of Euler angles to define the geometry. A body-fixed set of axes is used on the spinning object with the z axis being the axis of symmetry. The magnetometer is mounted so that its sensitive axis is parallel to the x axis of the body-mounted coordinates. To evaluate Eq. (4) we transform the magnetometer sensitivity vector $(K, 0, 0)$ in the body-fixed coordinates, to an inertial system. K is the sensitivity coefficient for the magnetometer.

We choose an inertial system with its z axis oriented along the constant direction of the vehicle's angular momentum, and with the Earth's magnetic field vector in its x–z plane. The conversion of the magnetometer sensitivity vector to the inertial system using the Euler angles is described by Hughes[10] and Thomson.[11]

Received March 14, 1994; revision received Sept. 17, 1996; accepted for publication Sept. 18, 1996. Copyright © 1996 by the American Institute of Aeronautics and Astronautics, Inc. All rights reserved.

*Consultant, Electrical Engineering.
†President. Associate Fellow AIAA.

The transformation is a series of three rotations as in the following matrix:

$$\begin{bmatrix} \cos\theta_s & \sin\theta_s & 0 \\ -\sin\theta_s & \cos\theta_s & 0 \\ 0 & 0 & 1 \end{bmatrix} \begin{bmatrix} \cos\gamma & 0 & \sin\gamma \\ 0 & 1 & 0 \\ -\sin\gamma & 0 & \cos\gamma \end{bmatrix} \times \begin{bmatrix} \cos\theta_p & \sin\theta_p & 0 \\ -\sin\theta_p & \cos\theta_p & 0 \\ 0 & 0 & 1 \end{bmatrix}$$

where

$\theta_s =$ spin angle
$\gamma =$ coning half-angle
$\theta_p =$ precession angle

We can write the magnetic field vector as

$$\boldsymbol{h} = H(\sin\beta, 0, \cos\beta) \tag{5}$$

where

$\beta =$ the angle between the vehicle total angular momentum vector and the local magnetic field vector
$H =$ magnitude of local magnetic field vector

In terms of the preceding definitions, Eq. (4) becomes

$$F_o = KH(\cos\theta_s \cos\gamma \cos\theta_p \sin\beta + \cos\theta_s \cos\beta \sin\gamma - \sin\theta_s \sin\theta_p \sin\beta) \tag{6}$$

To obtain the final desired form of the magnetometer output we write the following:

$$A = KH \qquad \theta_s = 2\pi\, f_s\, t_i + \phi_s \qquad \theta_p = 2\pi\, f_p\, t_i + \phi_p$$

Substituting these expressions in the equation for F_O gives the following result for the magnetometer estimation model:

$$F(\boldsymbol{\alpha}, t_i) = A\{\cos(2\pi f_s t_i + \phi_s)\cos(\gamma)\cos(2\pi f_p t_i + \phi_p)\sin(\beta) + \cos(2\pi f_s t_i + \phi_s)\cos(\beta)\sin(\gamma) - \sin(2\pi f_s t_i + \phi_s)\sin(2\pi f_p t_i + \phi_p)\sin(\beta)\} + V_o \tag{7}$$

where $\boldsymbol{\alpha} = (A, \beta, \gamma, f_s, \phi_s, f_p, \phi_p, V_o)$. Thus, the parameter set consists of eight elements as follows.

Magnetometer output amplitude coefficient:

$$\alpha_1 = A$$

Angle between vehicle total angular momentum vector and local magnetic field vector:

$$\alpha_2 = \beta$$

Vehicle coning half-angle:

$$\alpha_3 = \gamma$$

Vehicle spin rate relative to body-fixed coordinate system:

$$\alpha_4 = f_s$$

Vehicle spin phase angle relative to body-fixed coordinate system at sample block time zero:

$$\alpha_5 = \phi_s$$

Precession rate (coning rate) relative to inertial space:

$$\alpha_6 = f_p$$

Precession phase angle relative to inertial space at sample block time zero:

$$\alpha_7 = \phi_p$$

The dc offset of magnetometer:

$$\alpha_8 = V_o$$

Note that this analysis assumes that the magnetic field is constant over the trajectory interval examined. If the field cannot be considered constant, additional variables should appear in Eq. (5). For flight vehicles we have examined, the approximation appears to be valid, but other investigators are cautioned to consider its validity for their particular case.

Solving the Minimization Problem

Minimizing $z(\boldsymbol{\alpha})$ [Eq. (2)] with respect to $\boldsymbol{\alpha}$ using the model $F(\boldsymbol{\alpha}, t_i)$ [Eq. (7)] obtains the optimal solution to the estimation problem [Eq. (3)]. Thus, the problem can be stated as

$$z(\boldsymbol{\alpha}) = \min_{\alpha} z(\boldsymbol{\alpha}) \tag{8}$$

The nonlinear programming algorithm selected here to solve this minimization problem is the Davidon–Fletcher–Powell (DFP) algorithm.[5,9,12] Although no one nonlinear programming has been developed that will solve all problems, the DFP algorithm has been found to be very effective in a wide class of problems[13] and is generally recognized as being among the very best available, if not the best. The specific algorithmic code used is as described by Press et al.[14]

The DFP algorithm requires the gradient vector

$$\nabla_\alpha z(\boldsymbol{\alpha}) = \left[\frac{\partial z}{\partial \alpha_1}, \frac{\partial z}{\partial \alpha_2}, \ldots, \frac{\partial z}{\partial \alpha_8}\right] \tag{9}$$

Using the expression for z from Eq. (2), we find

$$\nabla_\alpha z(\boldsymbol{\alpha}) = \sum_{i=1}^{n} 2[F(\boldsymbol{\alpha}, t_i) - f(t_i)]\left[\frac{\partial F(\boldsymbol{\alpha}, t_i)}{\partial \alpha_1}, \ldots, \frac{\partial F(\boldsymbol{\alpha}, t_i)}{\partial \alpha_8}\right] \tag{10}$$

From the expression for $F(\boldsymbol{\alpha}, t_i)$ given in Eq. (7) and the accompanying definition of α, we find the following expressions for the partial derivatives:

$$\frac{\partial F}{\partial A} = \{\cos(2\pi f_s t_i + \phi_s)\cos(\gamma)\cos(2\pi f_p t_i + \phi_p)\sin(\beta) + \cos(2\pi f_s t_i + \phi_s)\cos(\beta)\sin(\gamma) - \sin(2\pi f_s t_i + \phi_s)\sin(2\pi f_p t_i + \phi_p)\sin(\beta)\} \tag{11}$$

$$\frac{\partial F}{\partial \beta} = A\{\cos(2\pi f_s t_i + \phi_s)\cos(\gamma)\cos(2\pi f_p t_i + \phi_p)\cos(\beta) - \cos(2\pi f_s t_i + \phi_s)\sin(\beta)\sin(\gamma) - \sin(2\pi f_s t_i + \phi_s)\sin(2\pi f_p t_i + \phi_p)\cos(\beta)\} \tag{12}$$

$$\frac{\partial F}{\partial \gamma} = A\{-\cos(2\pi f_s t_i + \phi_s)\sin(\gamma)\cos(2\pi f_p t_i + \phi_p)\sin(\beta) + \cos(2\pi f_s t_i + \phi_s)\cos(\beta)\cos(\gamma)\} \tag{13}$$

$$\frac{\partial F}{\partial f_s} = A\{-\sin(2\pi f_s t_i + \phi_s)\cos(\gamma)\cos(2\pi f_p t_i + \phi_p)\sin(\beta) - \sin(2\pi f_s t_i + \phi_s)\cos(\beta)\sin(\gamma) - \cos(2\pi f_s t_i + \phi_s)\sin(2\pi f_p t_i + \phi_p)\sin(\beta)\}2\pi t_i \tag{14}$$

$$\frac{\partial F}{\partial \phi_s} = A\{-\sin(2\pi f_s t_i + \phi_s)\cos(\gamma)\cos(2\pi f_p t_i + \phi_p)\sin(\beta) - \sin(2\pi f_s t_i + \phi_s)\cos(\beta)\sin(\gamma) - \cos(2\pi f_s t_i + \phi_s)\sin(2\pi f_p t_i + \phi_p)\sin(\beta)\} \tag{15}$$

$$\frac{\partial F}{\partial f_p} = A\{-\cos(2\pi f_s t_i + \phi_s)\cos(\gamma)\sin(2\pi f_p t_i + \phi_p)\sin(\beta) - \sin(2\pi f_s t_i + \phi_s)\cos(2\pi f_p t_i + \phi_p)\sin(\beta)\}2\pi t_i \quad (16)$$

$$\frac{\partial F}{\partial \phi_p} = A\{-\cos(2\pi f_s t_i + \phi_s)\cos(\gamma)\sin(2\pi f_p t_i + \phi_p)\sin(\beta) - \sin(2\pi f_s t_i + \phi_s)\cos(2\pi f_p t_i + \phi_p)\sin(\beta)\} \quad (17)$$

$$\frac{\partial F}{\partial V_o} = 1 \quad (18)$$

The minimization algorithm selected will find only a local minimum; therefore, reasonable initial conditions for the state (parameter) vector must be provided. If these are not carefully selected, the algorithm may find some local minimum far from the desired one. Examination of a plot of the magnetometer output vs time provides initial values for α_1, α_4, α_5, α_6, α_7, and α_8.

The initial estimate for $\alpha_3 = \gamma =$ vehicle coning half-angle can be determined from Eqs. (12), (15), and (30) in Hughes[10]:

$$\gamma = \cos^{-1}\left\{\frac{f_s}{(R-1)f_p}\right\} \quad (19)$$

where

$$R = I_x/I_z = I_y/I_z \quad (20)$$

i.e., R is the ratio of pitch to roll moments of inertia for the vehicle.

The ratio of pitch to roll moments of inertia is assumed known, at least approximately. The initial estimates for f_s and f_p are used in Eq. (19).

This leaves only $\alpha_2 = \beta$ to be assigned an initial value. Comparing the appearance of plots of $F(\alpha, t_i)$ vs time will aid the selection of an initial value of α_2.

Given the initial values as described, the algorithm will provide an optimal estimate $\hat{\boldsymbol{\alpha}}$ corresponding to the local minimum discovered.

An estimate is also available for the value of R, the ratio of pitch to roll moments of inertia, computed from the elements of $\hat{\boldsymbol{\alpha}}$ and Eq. (19); i.e.,

$$\hat{R} = \frac{\hat{f}_s}{\hat{f}_p \cos\hat{\gamma}} + 1 \quad (21)$$

The value of $\hat{R}$ found by Eq. (21) should be reasonably close to the vehicle design value.

A check on the credibility of the estimate $\hat{\boldsymbol{\alpha}}$ is the standard deviation for the estimate, which is

$$\sigma = \sqrt{z(\hat{\boldsymbol{\alpha}})/(n-1)} \quad (22)$$

The signal-to-noise ratio (SNR) can be written as

$$\text{SNR} = 20\log(\hat{A}/\sigma)\,\text{dB} \quad (23)$$

The SNR should be approximately the same as the design value for the magnetometer system.

An SNR resulting from a large value of σ indicates with high probability that an erroneous local minimum has been found and that more accurate initial values are required for the algorithm to converge to the desired minimum.

Example

Figure 1 shows a real magnetometer output (dotted values) from a laboratory fixture, which simulates spin and precession. The fixture was such that the equivalent total angular momentum vector was approximately vertical and the equivalent coning half-angle was about $\pi/4$ rad. A plot of the magnetometer output is shown in Fig. 1. Examination of the figure indicates that the values for spin rate and precession rate are about 0.5 and 0.0813 Hz. Because the coning half-angle γ was known to be about $\pi/4$ rad, the design value of R is found from Eq. (20) to be 8.7. The dip, or inclination of the Earth's magnetic field from the horizontal in the Tustin area where the test were concluded, is about 60 deg downward.[15,16] Therefore,

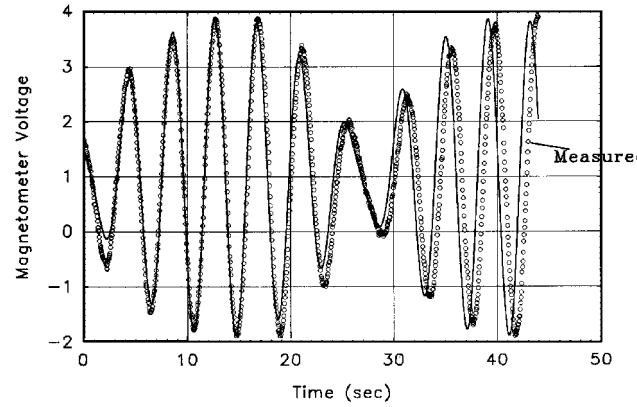

a) Initial guess at matching experimental data

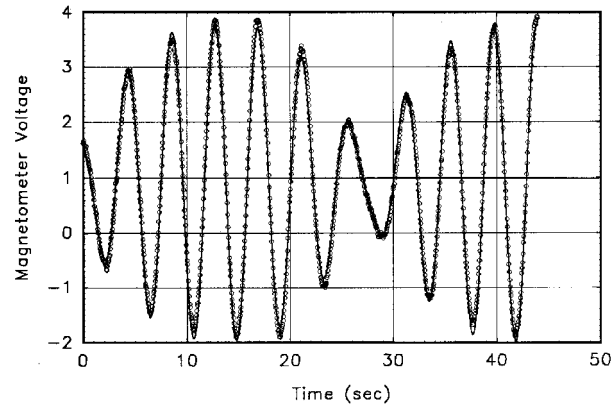

b) Match to data after optimization

Fig. 1 Experimental demonstration of parameter optimization.

the angle β between the total angular momentum vector and the local magnetic intensity vector was about 150 deg or 2.618 rad.

The equations presented in the preceding sections were solved numerically. The operation of the computer program was checked by creating a fictitious magnetometer data file based on the model previously described. Without additive noise the residual total square error $z(\hat{\boldsymbol{\alpha}})$ was very small and $\hat{\boldsymbol{\alpha}}$ was the same as the fictitious model parameters, indicating convergence of the algorithm. With additive noise in the magnetometer model data sequence, the SNR found by Eq. (23) was in good agreement with the known value. Because the fictitious data stream was generated by the estimation model, the tests just described check only the operation of the nonlinear programming algorithm, not the validity of the estimation model. The validity of the estimation model will be checked using real data from the magnetometer test fixture previously described.

For determining the initial estimate of the unknown parameters, we used a spreadsheet program. The magnetometer output, Eq. (7), was calculated for a priori estimates of the parameters. Direct comparison of the graphs of the actual data vs time to the calculated data allowed selection of the proper initial values by inspection. Figure 1a shows the result of this estimation for our laboratory model and is typical of the kind of agreement possible. The coning and spin frequencies are estimated first to get proper frequencies into the data. Then the phases are adjusted to get the proper shapes. This method could be automated, but for analysis of flight data after the fact that is not necessary.

Applying the estimation algorithm to the actual magnetometer data gave the results shown in Table 1. A plot of the magnetometer estimation model outputs are shown for the optimal parameter vector $\hat{\boldsymbol{\alpha}}$ in Fig. 1b. Figure 1b shows that the optimal parameter vector estimate $\hat{\boldsymbol{\alpha}}$ produces an estimation model output that closely matches the real magnetometer output. The validity of the estimation model is thus verified, at least qualitatively. Quantitative validation is evident from the SNR shown in Table 1 for the optimal estimate. The table shows SNR = 28.6 dB as compared to the known value of about 30 dB for the magnetometer.

Table 1 Magnetometer model parameter estimation

Parameter	Initial	Estimated
Spin rate, Hz	0.5000	0.4905
Pitch/roll inertia ratio	8.5000	9.4512
Precession rate, Hz	0.0813	0.0772
Coning half-angle, rad	0.7619	0.8332
SNR, dB	30.0000	28.5660
Spin phase angle, rad	3.9270	4.1693
Precession phase angle, rad	0.0000	0.2059
Peak signal, V	3.0000	2.9305
DC offset, V	1.0000	0.9171
Magnetic field angle, rad	2.6180	2.5825
Number of samples: 1100 at 55 Hz		

Deduction of Absolute Pointing Direction

A three-axis magnetometer has been used to obtain accurate pointing information for an intercontinental ballistic missile (ICBM) distance launch on the Inflatable Exoatmospheric Object (IEO) program[17] in 1972. More recently, highly accurate orientations were obtained on the Firefly sounding rocket launch in 1989. For Firefly, the uncertainty in orientation inherent with these devices was eliminated through the use of a sun sensor also, which provided a positioning pulse once during each spin cycle. As shown subsequently, similar information can be obtained with a single-axis magnetometer without the use of any additional inputs, relying on the variation of the Earth's magnetic field along the flight path. A similar approach was previously used for IEO data reduction for a three-axis magnetometer.[17] The details of this earlier approach by Massachusetts Institute of Technology, Lincoln Laboratory, personnel was never published in the open literature. The approach used here is similar but more comprehensively quantifies the resulting error.

As already shown, a single-axis magnetometer can be used to obtain the angle between the payload's angular momentum vector and the Earth's magnetic field by modeling the motion over a part of the trajectory. The result is that the payload's angular momentum vector is known to lie on a cone around the Earth's magnetic field vector.

At a later point in the trajectory, the direction of the Earth's magnetic field has changed, and if the payload's angular momentum vector is constant, the result will be a cone of uncertainty different from that found at the earlier point. This is shown in Fig. 2. The intersection of the two cones of uncertainty must contain the actual payload angular momentum vector. Thus, the cone of uncertainty has been reduced to a pair of possible orientation vectors. However, if the calculation is repeated for a third point along the trajectory, a third cone of uncertainty results that must also contain the payload angular momentum vector. When this cone is used together with the one from the earlier point a new pair of possible payload orientations is found. However, only one of this new pair will match one vector of the pair of vectors found from the first two trajectory points. This matching vector must be the actual payload angular momentum vector.

The case of a payload with a constant angular momentum over large portions of its trajectory is a common and usual situation. Furthermore, the analysis shows that the deduction of β, the angle between the payload's angular momentum vector and the Earth's magnetic field, is feasible by matching trajectory parameters over a 10-s portion of the flight. Because suborbital trajectories of interest range from about 500 s in duration for short sounding rocket flights, to 2400 s for ICBM flights, the opportunity exists to apply the cone-of-uncertainty analysis earlier highlighted to many points along the trajectory. Although only three points are theoretically needed, as already shown, many points will be useful to mitigate the effect of measurement errors on the analysis.

The purpose of this part of the paper is to show that the analysis highlighted can be used for realistic trajectories in the presence of measurement errors of the parameter beta. We show that there are conditions where the method will be of marginal usage, but many cases exist where absolute pointing data can be found from analysis of the single-axis magnetometer.

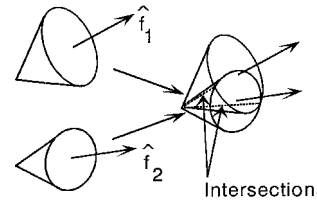

Fig. 2 Intersections of the cones of uncertainty contain the target orientation.

Table 2 Deduced cosines for 1% 1-σ error in β

521-s trajectory Launch latitude and longitude = (28°N, 80°W) Impact latitude and longitude = (27.4 deg, 79.9)	Actual	Using 10 points		Using 50 points	
M_x	0.5774	0.439	13.8%[a]	0.519	5.8%
M_y	0.5774	0.542	3.5	0.569	0.8
M_z	0.5774	0.654	7.7	0.595	1.8

[a]Resulting |%| error relative to unit vector.

Analysis Approach

We assume that the trajectory parameters (altitude vs time) and the direction of the Earth's magnetic field are known accurately. The effect we are investigating is the impact of the measurement error in β. To determine this effect over a range of typical conditions, we model the ballistic trajectory as given by the equation

$$r = \frac{1}{C + A\cos(\psi - \psi_o)} \tag{24}$$

where A and C are constants of the trajectory, r is the distance from the Earth's center, and ψ is the polar angle. The model of the Earth's magnetic field is that of a dipole, whose axis of symmetry is tilted from that of the Earth by the spherical polar angles $\theta_m = 11.5$ deg and $\phi_m = -69$ deg. Defining λ as the complement of Θ (the polar angle in the spherical coordinate system of the Earth's field), it is the latitude of the magnetosphere. The direction of the magnetic field dipole moment is then given by

$$\frac{B_r}{B} = \frac{-2\sin\lambda}{(1 + 3\sin^2\lambda)^{\frac{1}{2}}} \tag{25}$$

$$\frac{B_\Theta}{B} = \frac{-\cos\lambda}{(1 + 3\sin^2\lambda)^{\frac{1}{2}}} \tag{26}$$

This simple model allows the magnetic field direction along typical trajectories of interest to be easily estimated. The Appendix shows the derivation of the pointing direction given the cones of uncertainty for two different points along a trajectory. When this procedure is applied to data where the value of β defining the cones is known accurately, the actual payload pointing direction is obtained from the first three points along any trajectory. For the analysis reported, the values of β were assigned random errors along the trajectory, and the ability to again deduce the pointing direction of the payload was studied.

To aid in deduction of pointing, we had to smooth the resulting inaccurate β values by curve fitting with a curve of order 1, 2, or 3 (in general, order 2 worked best). This has the effect of averaging out much of the error introduced by the random errors in β.

For example, Fig. 3 shows a typical trajectory run during this analysis. Figure 4 shows the resulting β values for a particular pointing vector of the payload (direction cosines all equal). The figure also shows a resulting set of β assigned a random 1% error, and the second-order curve fit to these data.

Parametric Analysis

The following paragraphs present the results of the study.

Effect of Number of Intervals Used in the Calculations

Table 2 shows the effect of increasing the number of points calculated along a trajectory from 10 to 50. See the Appendix for definition of $\boldsymbol{M}$. The improvement in accuracy results from the additional averaging obtained by using more data points. For short trajectories,

Table 3 Deduced direction cosines for 1% 1-σ error in β; 10 points used on each trajectory

	Actual	Flight time 521 s from (28°, 80°) to (27.4°, 79.9°)		Flight time 635 s from (28°, 80°) to (25.8°, 74.7°)		Flight time 850 s from (28°, 80°) to (18.9°, 53.1°)		Flight time 1949 s from (28°, 80°) to (15.8°, 44.5°)	
M_x	0.5774	0.439	13.8%	0.552	2.5%	0.576	0.1%	0.575	0.2%
M_y	0.5774	0.542	3.5	0.562	1.5	0.570	0.7	0.567	1.0
M_z	0.5774	0.654	7.7	0.611	3.4	0.586	0.9	0.588	1.1

Table 4 Effect of measurement error on deduced direction cosines

	Trajectory time 1949 s; from (28°N, 80°W) to (15.8°N, 44.5°W) 10 trajectory points used						
	Actual	With 1% error		With 5% error		With 10% error	
M_x	0.5774	0.575	0.2%	0.578	0.1%	0.581	0.4%
M_y	0.5774	0.567	1.0	0.545	3.2	0.518	5.9
M_z	0.5774	0.588	1.1	0.605	2.8	0.625	4.8

Table 5 Deduced direction cosines for different orientations

	Trajectory time 521 s from (28°N, 80°W) to (27.4°N, 79.9°W) 1% 1-σ error in β, 10 trajectory points used									
	Actual	Deduced		Actual	Deduced		Actual	Deduced	Actual	Deduced	
M_y	0	−0.026	2.6%	0.7071	0.712	0.5%	0.7071	0.422[a]	0.7071	0.709	0.2%
M_y	0.7071	0.698	0.9	0	0.001	0.1	0.7071	0.460	0.7071	0.697	1.0
M_z	0.7071	0.650	5.7	0.7071	0.702	0.5	0	0.332	0.0705	0.092	2.1

[a] Averages of deduced vector are meaningless because of positive to negative switches (resulting from average of 0.7, 0.7, −0.7, etc.).

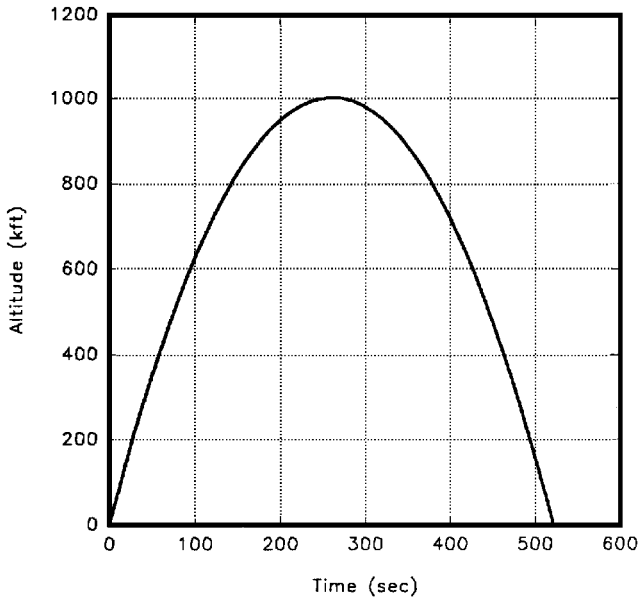

Fig. 3 Nominal trajectory (launch v = 7480 fps, launch azimuth = 75 deg from horizontal, launch latitude and longitude = 28° N, 80° W).

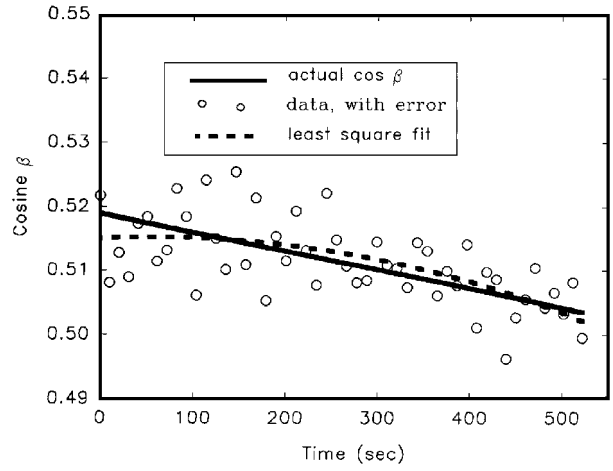

Fig. 4 Three methods of defining β, for nominal trajectory.

it may not be possible to use a sufficiently large number of points to get reasonable accuracy unless the spin and precession rates of the payload are sufficiently high to allow it.

Effect of Trajectory Length

One might expect that with a longer trajectory, the magnetic field direction will vary more, and the analysis will be less sensitive to errors in β (β will vary more strongly the more the magnetic field varies). Our calculations show that indeed this is correct. Table 3 presents deduced orientations as a function of the total time of the trajectory (from launch to impact), and the trend toward increasing accuracy with trajectory time is apparent, although for long times an asymptote is approached.

Effect of Magnitude of σ

For a long trajectory, it appears that the error in the deduced pointing direction is of the same order as the error in β. This is shown in Table 4, which shows the variation in σ from 1 to 10% for an ICBM trajectory. For shorter trajectories, or those using fewer points, the trend is the same, but the errors are greater than σ.

Effect of Vehicle Orientation

Table 5 shows that the analysis gives similar results if the angular momentum vector lies in either the xz or yz planes. If the orientation is in the xy plane, however, the effect of error in β can cause a switch in the deduced pointing vectors from positive to negative for some trajectory points. Thus, there remains an uncertainty for cases where the payload direction has no z component. However, if a small z component is introduced at a level about 10% of the x or y components, this ambiguity is removed.

Conclusions

What is believed to be a novel technique for obtaining dynamic data from a spinning spacecraft using only very simple onboard equipment has been demonstrated. Using only a relatively low-accuracy single-axis magnetometer we obtain reasonably accurate estimates for the vehicle spin rate, coning rate, coning half-angle, ratio of pitch to roll moments of inertia, angle between total angular momentum vector and local magnetic field intensity, and the magnitude of the local magnetic field intensity. The estimates are achieved

using a nonlinear programming solution of an optimal estimation problem formulation.

By processing the magnetometer data in successive blocks of a few hundred data points, it should be possible to obtain a sequence of estimates for time varying parameters. It should be necessary to manually initialize the estimation process only for the first data block because the remaining blocks can utilize the optimal estimate from the preceding block as the initial parameter vector.

Deduction of the absolute orientation of a spinning payload by using a single-axis magnetometer is feasible for a large variety of trajectories and orientations. To obtain reasonable accuracy 50 or more points along the trajectory should be analyzed. The longer the trajectory, the more accurate the magnetometer supplied data becomes.

Appendix: Deduction of Direction of Angular Momentum Vector

Let angular momentum have fixed orientation given by the unit vector

$$\boldsymbol{M} = M_x\,\hat{\boldsymbol{i}} + M_y\hat{\boldsymbol{j}} + M_z\hat{\boldsymbol{k}}$$

Let magnetic field direction at some point along flight path be given by the unit vector

$$\boldsymbol{f} = f_x\,\hat{\boldsymbol{i}} + f_y\hat{\boldsymbol{j}} + f_z\hat{\boldsymbol{k}}$$

Both unit vectors are defined in terms of a nonrotating Cartesian coordinate system with the z axis parallel to the Earth's spin axis, located at the payload position.

Let the half-angles of the two cones of uncertainty be β_1 and β_2 (see Fig. 2).

Let the general unit vector lying on the cone of uncertainty be given by

$$\boldsymbol{r} = x\hat{\boldsymbol{i}} + y\hat{\boldsymbol{j}} + z\hat{\boldsymbol{k}}, \qquad \text{where} \quad x^2 + y^2 + z^2 = 1 \tag{A1}$$

(procedure suggested by Kevin Davey, L'Garde, Inc.). We then know that

$$\boldsymbol{r}\cdot\boldsymbol{f} = \cos\beta_1 = xf_{x1} + yf_{y1} + zf_{z1} \tag{A2}$$

Similarly, for the next trajectory point

$$\cos\beta_2 = xf_{x2} + yf_{y2} + zf_{z2} \tag{A3}$$

Then from Eqs. (A2) and (A3)

$$x = \frac{\cos\beta_1 - yf_{y1} - zf_{z1}}{f_{x1}} = \frac{\cos\beta_2 - yf_{y2} - zf_{z2}}{f_{x2}} \tag{A4}$$

or

$$A - By - Cz = D - Ey - Fz \tag{A5}$$

where

$$A = \frac{\cos\beta_1}{f_{x1}}, \qquad B = \frac{f_{y1}}{f_{x1}}, \qquad C = \frac{f_{z1}}{f_{x1}}$$

$$D = \frac{\cos\beta_2}{f_{x2}}, \qquad E = \frac{f_{y2}}{f_{x2}}, \qquad F = \frac{f_{z2}}{f_{x2}}$$

Therefore,

$$(B - E)y = (F - C)z + (A - D)$$

or

$$y = Gz + H \tag{A6}$$

where

$$G = (F - C)/(B - E) \qquad \text{and} \qquad H = (A - D)/(B - E)$$

Also from Eqs. (A4–A6)

$$x = A - B\,(Gz + H) - Cz \tag{A7a}$$

or

$$x = Jz + K \tag{A7b}$$

where

$$J = -BG - C \qquad \text{and} \qquad K = A - BH$$

Substituting Eqs. (A6) and (A7) into Eq. (A1),

$$J^2z^2 + 2JKz + K^2 + G^2z^2 + 2GHz + H^2 + z^2 = 1$$

or

$$(J^2 + G^2 + 1)z^2 + (2JK + 2GH)z + (K^2 + H^2 - 1) = 0 \tag{A8}$$

The two possible solutions of Eq. (A8) produce the two lines of intersections between two cones. One of these values of r is equal to the angular momentum vector $\boldsymbol{M}$.

Ideally, a new set of points will give a different solution since $\boldsymbol{f}$ will change. However, one of the new solutions should equal one from the previous set of solutions because the solutions again contain $\boldsymbol{M}$, which is assumed to be constant.

In the presence of measurement errors, the new solution will not precisely match a previous one, but the set of solutions that from point to point is least variable is most likely to be, on average, $\boldsymbol{M}$.

References

[1]Rice, J. R., *The Approximation of Functions*, Vol. 1, Addison–Wesley, Reading, MA, 1964, pp. 2–7.

[2]Royden, H. L., *Real Analysis*, Macmillan, New York, 1963, pp. 97, 109–111, 157, 158.

[3]Kolmogorov, A. N., and Fomin, S. V., *Elements of the Theory of Functions and Functional Analysis*, Vol. 1, Graylock, Rochester, NY, 1957, pp. 16 ff, 77 ff.

[4]Porter, W. A., *Modern Foundations of Systems Engineering*, Macmillan, New York, 1966, pp. 46–50.

[5]Gue, R. L., and Thomas, M. E., *Mathematical Methods in Operations Research*, Macmillan, New York, 1968, pp. 117–125.

[6]Hadley, G., *Nonlinear and Dynamic Programming*, Addison–Wesley, Reading, MA, 1964.

[7]Mangasarian, O. L., *Nonlinear Programming*, McGraw–Hill, New York, 1969.

[8]Zangwill, W. I., *Nonlinear Programming*, Prentice–Hall, Englewood Cliffs, NJ, 1969.

[9]Polak, E., *Computational Methods in Optimization*, Academic, New York, 1971, pp. 56–66.

[10]Hughes, P. C., *Spacecraft Attitude Dynamics*, Wiley, New York, 1986, pp. 96–103.

[11]Thomson, W. T., *Introduction to Space Dynamics*, Dover, New York, 1986, pp. 33–37.

[12]Davidon, W. C., "Variable Metric Method for Minimization," *SIAM Journal on Optimization*, Vol. 1, No. 1, 1991, pp. 1–17.

[13]Colville, "A Comparative Study on Nonlinear Programming Codes," IBM New York Scientific Rept. 320-2949, June 1968.

[14]Press, W. H., Flannery, B. P., Teukolsky, S. A., and Vetterling, W. T., *Numerical Recipes: The Art of Scientific Programming*, Cambridge Univ. Press, New York, 1986.

[15]Hodgman, C. D. (ed.), *Handbook of Chemistry and Physics*, 44th ed., Chemical Rubber Publishing, 1963, p. 2762.

[16]Merrill, R. T., and McElhinney, M. W., *The Earth's Magnetic Field: Its History, Origin, and Planetary Perspective*, Academic, New York, 1983, p. 19, Fig. 2.2(b).

[17]McPhie, J. M., "IEO Final Flight Test Report," Massachusetts Inst. of Technology, Lincoln Lab. Project Rept. PA 356, Cambridge, MA, Oct. 1975.